

Resistive Switching in Memristors Based on Artificially Stacked Chemical-Vapor-Deposited Hexagonal-Boron Nitride

Lukas Völkel¹, Dennis Braun¹, Melkamu Belete¹, Satender Kataria¹, Thorsten Wahlbrink², and Max C. Lemme^{1,2}

¹ Chair of Electronic Devices, RWTH Aachen University, Otto-Blumenthal-Str. 2, 52074 Aachen, Germany

² AMO GmbH, Advanced Microelectronic Center Aachen, Otto-Blumenthal-Str. 25, 52074 Aachen, Germany

Email: max.lemme@rwth-aachen.de / Phone: +49 241 802 0281

Abstract — Vertical nickel-hexagonal boron nitride (hBN)-nickel memristive devices based on mechanically stacked monolayer hBN are fabricated and electrically characterized. The devices reveal threshold resistive switching behavior. Comparative electrical measurements in air and vacuum indicate an influence of the measurement conditions on the cycle-to-cycle variability of the devices.

I. INTRODUCTION

Two-dimensional (2D) materials, in particular transition metal dichalcogenides and hexagonal boron nitride (hBN), are being investigated for their potential application as memristors in neuromorphic computing hardware [1, 2]. Chemical vapor deposited (CVD) multilayer hBN has been shown to exhibit volatile threshold resistive switching (RS) in two-terminal devices for emulating synaptic functions [3]. Here, we report on the RS behavior observed in memristors based on mechanically stacked hBN monolayers and the influence of measurement conditions on the cycle-to-cycle variability of the devices.

II. DEVICE FABRICATION

Commercial, CVD grown hBN monolayers on copper foil have been used to fabricate two-terminal memristive devices. The electrodes have been formed via DC-sputtering of 55 nm nickel (Ni) and lift-off. The h-BN layers have been mechanically stacked via a wet-etching transfer process, where one monolayer with supporting polymer is manually placed on a second monolayer to obtain bilayer hBN (process details similar to [4]). The fabrication process and the resulting device schematic are shown in **Fig. 1**. The characteristic Raman peak was found at $1367 \pm 0.5 \text{ cm}^{-1}$ with different peak amplitudes (**Fig. 2**), indicating spatial variations in the hBN thickness [5]. Scanning electron microscope images support this assumption (**Fig. 3**) and reveal sites with multiple layers.

III. RESULTS AND DISCUSSION

Current-voltage (I-V) measurements have been conducted in air and in vacuum. First, a voltage sweep in the negative direction has been applied, followed by a voltage sweep in the positive direction with maximum voltages of $|V| = 2.8 \text{ V}$. Current compliance (cc) has

been set to avoid damage to the devices in the low resistive state (LRS). **Figs. 4-6** depict comparative sets of I-V sweeps in ambient air, vacuum and again ambient air. Each set consists of 10 switching cycles with a cc of 50 nA. The I-V curves are plotted in grey, while the average of the 10 cycles is plotted in red (**Figs. 4a, 5a, 6a**). The device exhibits threshold RS [6]. It is observed that V_{SET} decreases in vacuum compared to that in air. In addition, the variability of the switching process increases in vacuum (**Fig. 5a**), which is reflected by an oscillating behavior of the current during the LRS transition. More stable switching behavior is recovered again after exposing the sample to air (**Fig. 6a**). The voltages corresponding to a fixed current value of 25 nA were extracted from each cycle for statistical analyses (**Figs. 4b, 5b, 6b**). In vacuum, no visible distinction between LRS and HRS is observed, which reflects the large variability addressed above (**Fig. 5b**). This oscillating behavior is not visible in ambient air conditions conducted before and after the vacuum measurements (**Figs. 4b, 6b**). The decrease of V_{SET} may be explained by the removal of interfacial water between the hBN and the Ni electrodes which otherwise gives rise to a dielectric screening effect [7]. The change in the cycle-to-cycle variability between air and vacuum measurements may further indicate an additional influence of air molecules on the switching behavior of the hBN memristors.

ACKNOWLEDGMENT

Funding by the German BMBF (NEUROTEC, 16ES1134) and the European Commission (QUEFORMAL, 829035) is gratefully acknowledged.

REFERENCES

- [1] M. Belete et al., *Adv. Electron. Mater.* 6, 1900892 (2020).
- [2] S. Chen et al., *Nat. Electron.* 3, 638–645 (2020).
- [3] Y. Shi et al., *Nat. Electron.* 1, 458–465 (2018).
- [4] H. Pandey et al., *Ann. Phys.* 529, 1700106 (2017).
- [5] R. V. Gorbachev et al., *Small.* 7, 465–468 (2011).
- [6] M. Lanza et al., *Adv. Electron. Mater.* 5, 1800143 (2019).
- [7] B. Wang et al., *Cryst. Res. Tech.* 53, 1800006 (2018).

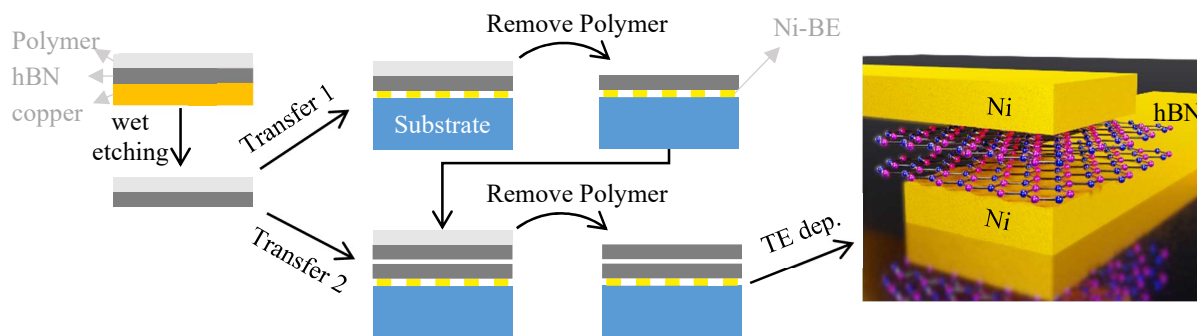


Fig. 1 Fabrication process flow and resulting schematic of vertical Ni-hBN-Ni memristors. BE: bottom electrode, TE dep.: top electrode deposition. Bottom electrode deposition not shown.

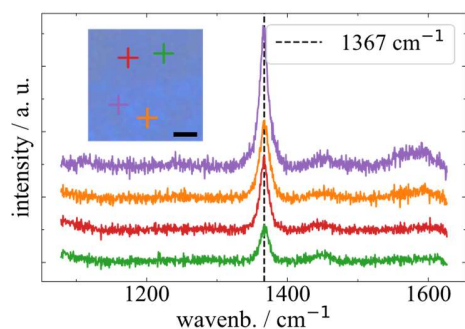


Fig. 2 Raman spectra of stacked hBN film. The characteristic hBN peak can be found at 1367 cm^{-1} . Inset: Microscope image with measurement positions (scale bar: $2\text{ }\mu\text{m}$).

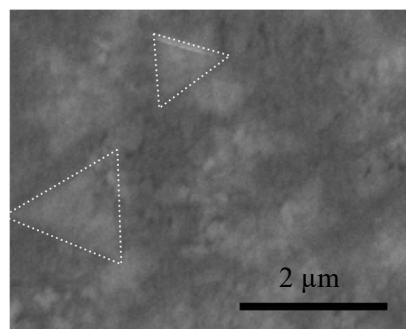


Fig. 3 SEM image of bilayer hBN after transfer. Bright areas (marked) are sites with fewlayer hBN.

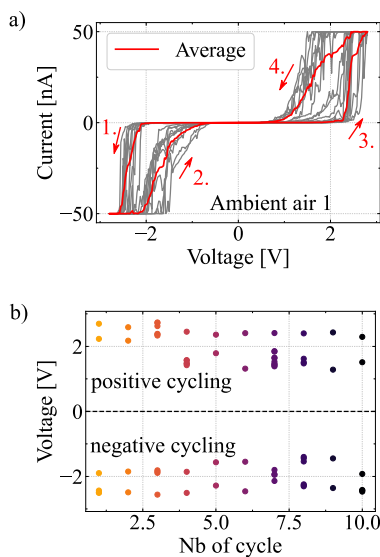


Fig. 4 (a) 10 I-V cycles in ambient condition. The red curve shows the average I-V cycle. (b) Statistics of voltage at half of cc (25 nA).

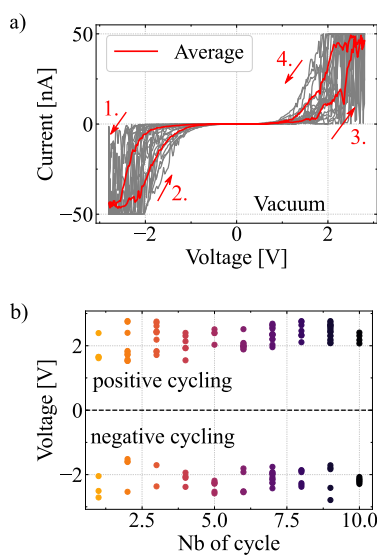


Fig. 5 (a) 10 I-V cycles in vacuum condition and (b) statistics. Increase of cycle-to-cycle variability and oscillation of the current in most cycles visible.

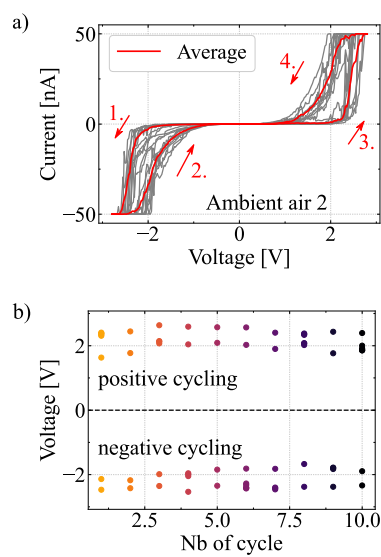


Fig. 6 (a) 10 I-V cycles in ambient conditions after vacuum measurements and (b) statistics. Switching window is recovered and oscillations are suppressed.